

MAGNETAR-LIKE ACTIVITY FROM THE CENTRAL COMPACT OBJECT IN THE SNR RCW103

N. REA^{1,2}, A. BORGHESE¹, P. ESPOSITO¹, F. COTI ZELATI^{1,3,4}, M. BACHETTI⁵, G. L. ISRAEL⁶, A. DE LUCA⁷
Draft version July 15, 2016

ABSTRACT

The 6.67 hr long periodicity and the variable X-ray flux, of the central compact object (CCO) at the center of the SNR RCW 103, named 1E 161348–5055, have been always difficult to interpret within the standard scenarios of an isolated neutron star or a binary system. On 2016 June 22, the Burst Alert Telescope (BAT) onboard *Swift* detected a magnetar-like short X-ray burst from the direction of 1E 161348–5055, also coincident with a large long-term X-ray outburst. Here we report on the properties of this magnetar-like burst, on the *Chandra*, *NuSTAR*, and *Swift* (BAT and XRT) observations of this peculiar source during its 2016 outburst peak, as well as on the study of its long-term X-ray outburst activity (from 1999 to July 2016). We find that all the X-ray properties of this object are perfectly in line with it being a magnetar, which undergoes typical X-ray flares and transient events. However, in this scenario, the 6.67 hr periodicity can only be interpreted as the rotation period of this strongly magnetized neutron star, which would represent by orders of magnitudes the slowest pulsar ever detected. We briefly discuss the different slow-down viable scenarios, favouring a picture involving a period of fall-back accretion after the supernova explosion, similarly to what invoked (although in a different regime) to explain the “anti-magnetar” scenario for other CCOs.

Keywords: X-rays: stars — stars: neutron — stars: individual (1E 161348–5055; RCW103)

1. INTRODUCTION

The central compact object (CCO) 1E 161348–5055, laying within the supernova remnant (SNR) RCW 103, has been a mysterious source all along. Despite being presumably an isolated neutron star (NS), hence allegedly a stable source, it shows long-term X-ray outbursts lasting several years, where its luminosity increases by a few orders of magnitude, as well as a very peculiar ~ 6.67 hr periodicity with an extremely variable profile along different luminosity levels (De Luca et al. 2006). Several interpretations on the nature of this system have been proposed since more than a decade, from an isolated slowly spinning magnetar with a substantial fossil-disk to a young low mass X-ray binary system, or even a binary magnetar, but none of these interpretations is straightforward, nor they could explain the overall observational properties of this peculiar system (Garmire et al. 2000; De Luca et al. 2006, 2008; Li 2007; Pizzolato et al. 2008; Bhadkamkar & Ghosh 2009; Esposito et al. 2011; Liu et al. 2015; Popov, Kaurov & Kaminker 2015).

A millisecond burst from a region overlapping the SNR RCW 103 triggered the *Swift* Burst Alert Telescope

(BAT) on 2016 June 22 at 02:03 UT (D’Ai et al. 2016). These short X-ray bursts are a peculiar characteristic of the soft gamma repeater (SGR) and anomalous X-ray pulsar (AXP) classes, believed to be isolated NSs powered by the strength and instabilities of their 10^{14-15} G magnetic fields (aka magnetar; Duncan & Thompson 1992; Mereghetti 2008; Turolla, Zane & Watts 2015). In this work, we report on the analysis of the magnetar-like burst detected by BAT and on new simultaneous *Chandra* and *NuSTAR* observations performed soon after the BAT burst trigger during the outburst peak of the source (§ 2). Furthermore, we put our results in the contest of the long-term *Swift*, *Chandra*, and *XMM-Newton* monitoring campaigns of 1E 161348–5055 from 1999 until 2016 July (§ 3). We then discuss our findings and the derived constraints on the nature of this puzzling object (§ 4).

2. X-RAY OBSERVATIONS AND DATA ANALYSIS

2.1. Swift

The *Swift* data were processed and analysed with usual procedures using the standard tasks included in the HEASOFT software package (v.6.19) and the calibration files in the 2016-05-02 CALDB release. The *Swift* X-ray Telescope (XRT) source counts were extracted from a circular region centered on the source position, and with a radius of 10 pixels (1 pixel corresponds to $2.36''$), and the background events from an annulus of inner and outer radius of 10 and 20 pixels, respectively. Only the observation soon before the BAT trigger, which yielded a severe pile-up, had to be extracted differently. In this case we modeled the wings of the radial profile of the source point-spread function (PSF) with a King function (Moretti et al. 2005), extrapolated the model back to the core of the PSF, and excised the inner 3.5 pixels of the extraction region. We grouped the background-subtracted spectra so to have at least 20 counts per energy channel, and fitted them jointly within XSPEC v.12.9 (which was used

¹ Anton Pannekoek Institute for Astronomy, University of Amsterdam, Postbus 94249, NL-1090 GE Amsterdam, the Netherlands. Email: rea@ice.csic.es. The first four authors equally contributed to this work.

² Institute of Space Sciences (IEEC–CSIC), Carrer de Can Magrans S/N, 08193 Barcelona, Spain.

³ Università dell’Insubria, via Valleggio 11, I-22100 Como, Italy

⁴ INAF–Osservatorio Astronomico di Brera, via Bianchi 46, I-23807 Merate (LC), Italy

⁵ INAF–Osservatorio Astronomico di Cagliari, località Poggio dei Pini, strada 54, I-09012 Capoterra (CA), Italy

⁶ INAF–Osservatorio Astronomico di Roma, via Frascati 33, 00040, Monteporzio Catone (RM), Italy

⁷ INAF–Istituto di Astrofisica Spaziale e Fisica Cosmica Milano, Via E. Bassini 15, I-20133 Milano, Italy

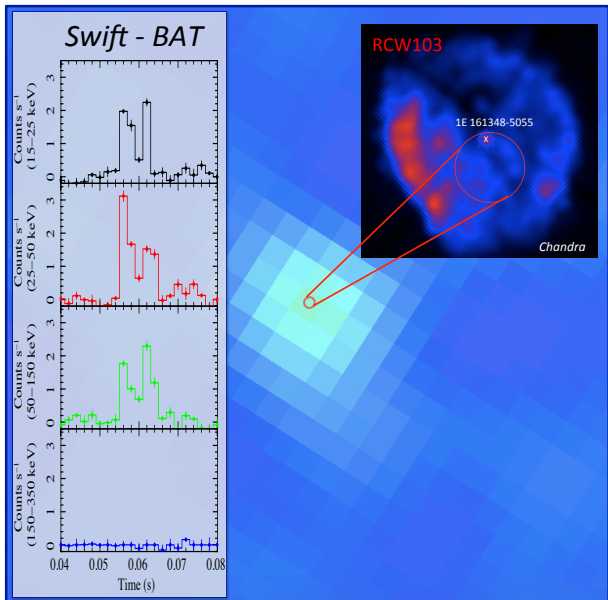


Figure 1. We show the *Swift*-BAT image of the burst detected on 2016 June 22 with over imposed the burst light curves at different energies (bin size: 2 ms) and a *Chandra* ACIS-I image of the SNR RCW 103 and its central source (white cross), 1E 161348–5055. The red 1.5′ circle is the positional accuracy of the detected burst (see text for details).

for all spectral analysis presented in this work), limiting our analysis to the 1–10 keV energy range.

We analysed the *Swift*-BAT data relative to the burst. The T90 duration of the event (i.e., the time during which 90% of the burst counts were collected) was 0.009 ± 0.001 s and its total duration was ~ 10 ms. These durations were computed by the Bayesian blocks algorithm BATTBLOCKS on mask-weighted light curves binned at 1 ms in the 15–150 keV, where essentially all the emission is contained. The BAT mask-tagged light curves, images and spectra were created only for the burst event (trigger 700791, obs.ID 00700791000). We extracted a 15–150-keV sky image and performed a blind source detection over the whole duration of the burst: a single, point-like source was detected at high significance (14.5σ) at the best-fit coordinates R.A. = $16^{\text{h}}17^{\text{m}}29^{\text{s}}62$, Decl. = $-51^{\circ}03'07''.9$, with an uncertainty radius of 1.5 arcmin (1σ , including a systematic error of 0.25 arcmin; see Tueller et al. 2010). This position is consistent with a single known X-ray source: 1E 161348–5055. Together with the exceptionally high flux of 1E 161348–5055 at the epoch of the burst, this clinches the case of the X-ray source in RCW 103 as the origin of the burst.

2.2. Chandra

After the burst trigger, 1E 161348–5055 was observed with the Advanced CCD Imaging Spectrometer spectroscopic array (ACIS-S; Garmire et al. 2003) on board the *Chandra X-Ray Observatory* starting on 2016 June 25 at 09:20:07 and until 22:00:38 UT, for an on-source exposure time of 44.2 ks (obs ID: 18878). The ACIS-S was configured in continuous clocking (CC) mode with FAINT telemetry format, yielding a readout time of 2.85 ms at the expense of one dimension of spatial information. The source was positioned on the back-illuminated S3 chip.

We analysed the data following the standard analysis

threads⁸ with the *Chandra* Interactive Analysis of Observations software (CIAO, v. 4.8; Fruscione et al. 2006) and the calibration files stored in the *Chandra* CALDB (v. 4.7.2). We accumulated the source photon counts within a box of dimension 3×3 arcsec² centered on the most accurate position of the target, RA = $16^{\text{h}}17^{\text{m}}36^{\text{s}}.23$, Dec = $-51^{\circ}02'24''.6$ (De Luca et al. 2008). The background was estimated by collecting photons within two rectangular regions oriented along the readout direction of the CCD, symmetrically placed with respect to the target and both lying within the remnant, whose spatial extension is ~ 9 arcmin in diameter (Frank, Burrows & Park 2015). The average source net count rate was 3.352 ± 0.009 counts s⁻¹, which guarantees no pile up issues in the data set.

We also analysed in a similar way all the archival *Chandra* observations pointing at $<30''$ from our target (see Fig. 3), although for TE mode observations we extracted the photons from a $2''$ circular region, and the background from an annular region with radii 4– $10''$. These observations were used for the timing and spectral long-term analysis (see also below). When necessary, we corrected for pile up effects by using the model by Davis (2001).

2.3. NuSTAR

The *Nuclear Spectroscopic Telescope Array* mission (*NuSTAR*; Harrison et al. 2013) observed 1E 161348–5055 starting on 2016 June 25 at 06:46:47 UT and until June 26 at 18:42:50 UT, for a total on-source exposure time of 70.7 ks (obs ID: 90201028002), most of which simultaneously with the *Chandra* observation (§ 2.2). The data were processed using version 1.6.0 of the *NuSTAR* Data Analysis Software (NUSTARDAS), and the instrumental calibration files from 2016-05-02 CALDB (using the version 59 of the clock file to account for drifts in the *NuSTAR* clock caused by temperature variations). We used the tool NUPIPELINE with the default options for good time interval filtering to produce cleaned event files, and removed time intervals corresponding to passages through the South Atlantic Anomaly. We ran the NUPRODUCTS script to extract light curves and spectra and generate instrumental response files separately for FPMA and FPMB. We collected the source counts within a circular region of $30''$ radius, the background subtracted source count rate in the 3–79 keV was 0.21 ± 0.04 counts s⁻¹. We chose such a small extraction region for the source counts to limit the contamination from the SNR and to avoid a large region contaminated by ghost rays that extends up to $\sim 40''$ from the source. Background was estimated from two $60''$ circular regions in the same chip, one inside and one outside the ghost rays-contaminated area. We verified that the two background estimations did not produce a significantly different spectral modeling.

3. RESULTS

3.1. Burst properties

The light curve of the *Swift*-BAT burst shows a double-peak profile (Fig. 1). We fit the time-averaged spectrum extracted from the total duration of 10 ms with simple single-component models typically used for magnetar

⁸ See <http://cxc.harvard.edu/ciao/threads/pointlike>.

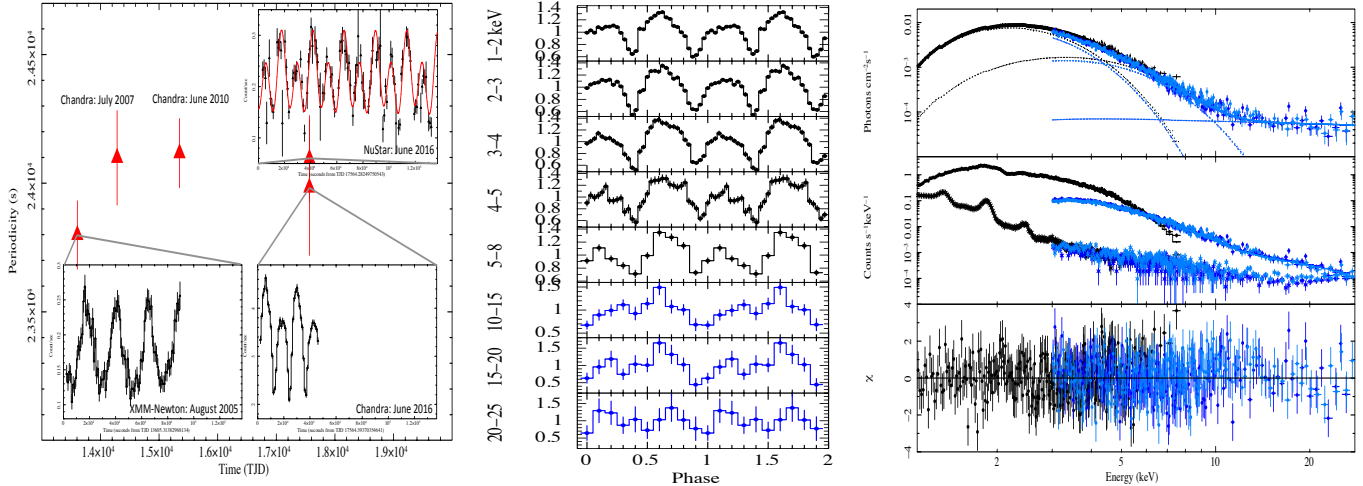


Figure 2. *Left:* Period determination for the longest available X-ray observations in the archive, with superimposed the light curve binned at 1 ks/bin. *Middle:* Energy dependent folded light-curve for the simultaneous *Chandra* and *NuSTAR* observations soon after the burst. *Right:* Simultaneous spectral fit of the *Chandra* (black) and *NuSTAR* (light and dark blue) data with two absorbed blackbodies and a power-law component.

bursts: a power law, a blackbody, and an optically-thin thermal bremsstrahlung (e.g., Israel et al. 2008). Only the blackbody model provided an acceptable fit, with a reduced χ^2 , $\chi^2_{\nu} = 1.06$ for 56 degrees of freedom (dof) and temperature $kT = 10.2 \pm 0.7$ keV (all errors are given at 1σ confidence level here and throughout the paper). The corresponding flux is $(1.9 \pm 0.2) \times 10^{-7}$ erg cm $^{-2}$ s $^{-1}$ in the 15–150 keV range (corresponding to a luminosity of 2.5×10^{38} erg s $^{-1}$ at 3.3 kpc). As suggested by the energy-resolved light curve (Fig. 1), the second peak is weaker and has a softer spectrum than the first one. The first ~ 5 ms of the event can be fit by a blackbody with $kT = 9.2 \pm 0.9$ keV, while for the second peak the blackbody temperature is $kT = 6.0 \pm 0.6$ keV.

3.2. Timing analysis

For the timing analysis, all photon arrival times were reported to the Solar System barycentre frame, using the DE200 ephemerides and the *Chandra* position (De Luca et al. 2008). First, we started a blind search for any fast periodic and aperiodic signals using our new *Chandra* and *NuSTAR* data sets, using the XRONOS timing package as well as the Z_n^2 test (Bucheri et al. 1983). We did not find any periodic signal via a Fourier transform, and we could detect in both observations only the known ~ 6.67 hr periodic modulation in the light curve (see Fig. 2). Furthermore, we also searched for periodic signals by assuming the 6.6 hr modulation as the orbital period, and correcting the time series for the Doppler shift that such an orbit might cause to any shorter periodic signal, but with no success. We inferred 3σ pulsed fraction upper limits for fast periodic signals (as explained in Israel & Stella 1996), of 5% (0.01–10 Hz), 6% (10–100 Hz) and in the 7–9% range for the highest sampled frequencies (100–200 Hz), for the *Chandra* observation. A similar analysis carried out on the *NuSTAR* data resulted on 3σ upper limits of 12% (0.01–3 Hz), and in the range 26–34% at higher frequencies (3–1000 Hz).

The light curve of the *NuSTAR* data (the longest continuous dataset for 1E161348–5055) is well fitted by two sinusoidal functions with fundamental period

24095 ± 167 s (at TJD 17565.0), and compatible periodicities adequately fit also the simultaneous *Chandra* data (23983 ± 263 s at TJD 17564.7; see Fig. 2)

In addition to the new observations, in search for a period derivative or any variability of the long term modulation, we re-analysed all available *Chandra* observations (at the time of writing) longer than 18 ks (7 observations), and the two archival *XMM-Newton* observations (De Luca et al. 2006). We performed a phase fitting analysis trying to follow the temporal evolution of the phases, but could not find a coherent timing solution due to the sparse observations. In Fig. 2 we show the best determinations of the ~ 6.67 hr period using the longest available datasets, as well as the profile of the periodicity for the two most extreme cases of a pure single peak (in 2005; De Luca et al. 2006), and a clear double peak (in June 2016; this paper). We also studied the variability of the profile as a function of the energy in the 1–25 keV energy, and found that the first peak is significantly softer than the second.

3.3. Spectral analysis

We started the spectral analysis by fitting simultaneously the new *Chandra* and *NuSTAR* observations (see Fig. 2; the source is detected above the background from 1.1–28 keV). We found that although the *Chandra* spectrum alone is well fit with two blackbodies, this is not the case when taking into account also the *NuSTAR* hard X-ray spectrum of the 1E161348–5055. Best joint fit is found for a model comprising of two absorbed ($N_H = 2.05(5) \times 10^{22}$ cm $^{-2}$) blackbodies with temperatures of $kT_1 = 0.53 \pm 0.01$ keV and $kT_2 = 1.00 \pm 0.05$ keV with radii (assuming a 3.3 kpc distance hereafter: Caswell et al. 1975) of $R_1 = 2.7 \pm 0.7$ km and $R_2 = 0.4 \pm 0.2$ km, plus the addition of a power-law component with photon index $\Gamma = 1.20 \pm 0.25$ (adding a constant between the two instruments to account for inter-calibration uncertainties, which was always within 10%). The total observed flux in the 0.5–30 keV energy range is $(3.7 \pm 0.1) \times 10^{-11}$ erg cm $^{-2}$ s $^{-1}$, and the joint fit gives $\chi^2_{\nu} = 1.11$ (660 dof).

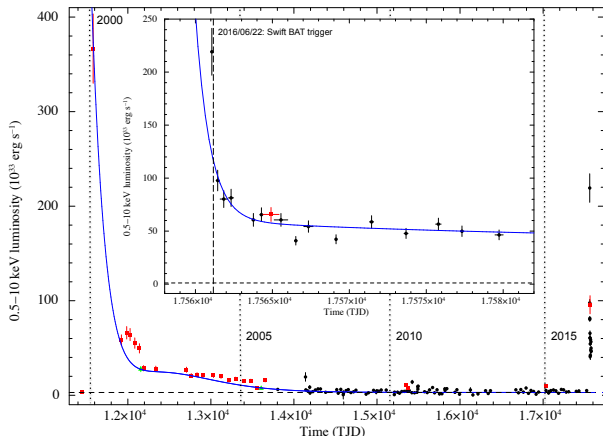


Figure 3. Long-term 0.5–10 keV luminosity history of 1E 161348–5055 as observed since 1999 until July 2016 by *Chandra* (red squares), *XMM-Newton* (green triangles) and *Swift* (black circles). Dashed line represents the source quiescent luminosity. The inset is a zoom of the 2016 outburst.

3.4. Outburst history

To study the outburst history of 1E 161348–5055, we re-analysed all the available *Chandra*, *XMM-Newton*, and *Swift* data of the source acquired from 1999 until 2016 July (see Fig. 3). All spectra were fitted by fixing the absorption column density to the best value derived using *Chandra* ($N_{\text{H}} = 2 \times 10^{22} \text{ cm}^{-2}$) plus two blackbody components (because at these soft energies the power-law is not required by the fit). We show the extrapolated 0.5–10 keV luminosity in Fig. 3. The source showed two outbursts in the past ~ 17 years, empirically fitted with a constant plus 3 exponential decays, and having a total (impulsive plus persistent) emitted energy in the 0.5–10 keV band of $E_{1st-out} \sim 9.9 \times 10^{42} \text{ erg}$ and $E_{2nd-out} \sim 1.6 \times 10^{42} \text{ erg}$ (extrapolating at when it will reach quiescence in about a year time). Both outbursts are characterised by the heating of two different regions on the surface, the first one that evolved from the outburst peak until quiescence from $kT_1 \sim 0.6\text{--}0.4 \text{ keV}$ ($R_1 \sim 5 - 1 \text{ km}$), while the second one (very dim in quiescence) from $kT_2 \sim 1.4\text{--}0.7 \text{ keV}$ ($R_2 \sim 1.4 - 0.1 \text{ km}$). As we observed in this work for the first time, at $> 6 \text{ keV}$ during the outburst peak, a non-thermal component is also present, and certainly pulsed until $\sim 20 \text{ keV}$.

4. DISCUSSION

We report on the first discovery of a magnetar-like short burst from a CCO, and study its coincident X-ray outburst activity. This short ms-burst and its spectrum, the outburst energetic, spectral decomposition and cooling (see § 3) are perfectly in line with what observed in magnetar outbursts (see Rea & Esposito 2011; Pons & Rea 2012). Furthermore, the non-thermal component that we observed with *NuSTAR* is also very typical, and will most probably fade quickly during the outburst decay. Magnetar outbursts are expected to be produced by the instability of strong magnetic bundles that stress the crust (from inside or outside; Perna & Pons 2011; Pons & Rea 2012; Beloborodov 2009) heating the surface in one or more regions, and at different depth inside the NS crust (than then drives how long the outburst will last each time). The high density of electrons in these

bundles might also cause resonant cyclotron scattering of the seed thermal photons, creating non-thermal high-energy components in the spectrum (that might be transient if the untwisting of these bundles during the outburst decay produces a decrease in the scattering optical depth). Furthermore, magnetospheric re-arrangements are expected during these episodes, that are believed to be the cause of the short X-ray bursts (see Turolla, Zane & Watts (2015) for a review). Repeated outbursts on an yearly timescale have also been detected before (i.e. 1E 1048.1–5937 or 1E 1547–5408; Bernardini et al. 2011; Kuiper et al. 2012; Archibald et al. 2015), and their recurrence time is expected to be related to the source magnetic strength, configuration and the NS age (see Perna & Pons 2011; Viganó et al. 2013).

In this scenario, the only puzzling property of 1E 161348–5055, that makes it unique among any SGR, AXP, CCO or other known NS, is the 6.67 hr long periodicity (which would represent the longest spin period ever detected in any pulsar, even considering slow pulsars in high mass X-ray binaries). On the other hand, the extreme variability of the modulation in time and energy, strongly disfavour the 6.67 hr modulation being due to an orbital period (see detailed discussion in De Luca et al. 2008; but see also Pizzolato et al. 2008), while again are fully consistent with the usual pulse profile variability observed in magnetars during flaring activity (see i.e. the cases of SGR 0501+4516, SGR 0418+5729, and CXOU J1647–4552; Rea et al. 2009, 2013; Rodríguez Castillo et al. 2014).

Isolated pulsar spin periods are observed to be limited to $\sim 12 \text{ s}$, with the slowest pulsars being indeed the magnetars. This period distribution is explained as due to magnetic field decay during the evolution of these neutron stars (see Pons, Viganó & Rea 2013). If we consider the slowest isolated pulsar that magnetic-field decay might produce, by means of the 2D code from Viganó et al. (2013), by assuming only core-field, no crustal impurity, an initial field ranging from 10^{13-15} Gauss , and a typical spin period at birth in the range of 1–300 ms, we cannot anyhow reproduce periods longer than $\sim 30\text{--}50 \text{ s}$.

Given the magnetar nature of the X-ray emission of this source, we are now left with discussing all possible slow down mechanisms other than the typical pulsar dipolar loss, to explain how a magnetar within a SNR with an age estimate of 2.2 kyr (Carter et al. 1997) could have ended up with such a long spin period. Since its discovery, many authors already discussed several scenarios (see De Luca et al. 2006; Li 2007; Pizzolato et al. 2008; Bhadkamakar & Gosh 2009; Lui et al. 2015; Popov, Kaurav, & Kamiker 2015), which we cannot summarize here, however we will highlight and discuss the possibilities that remains open, with their possible open issues.

First possibility might be a long-lived fossil disks (Chatterjee, Hernquist & Narayan 2000) that forms via the circularisation of fall-back material after the Supernova explosion (see i.e. De Luca et al. 2006; Li 2007). This might result in slowing down substantially the spin period. However, recent studies on the formation of fossil disks apparently disfavour their existence around NSs under reasonable assumption on the magnetic torque in the pre-SN phase (Perna et al. 2014), and indeed these fossil disks have been searched for decades around pul-

sars without a real conclusive detection yet. On the other hand, the magnetar flaring activity would most probably blow off such thin disks very quickly. Furthermore, in this scenario it would not be straightforward to understand what would make 1E161348–5055 different at formation from all other known pulsars (especially when associated with a relatively standard SNR; Frank, Burrows & Park 2015).

Another possibility is a magnetar in a low mass X-ray binary with an M6 (or later; De Luca et al. 2008) companion, emitting as if it was isolated, but that had the spin period tidally locked to the orbital motion of the system (see i.e. Pizzolato et al. 2008). However, also in this case an extreme fine-tuning is needed to explain how a very low mass companion remains bounded to the magnetar after a SN explosion.

The most viable interpretation we see, especially because perfectly in line with what proposed for other CCO systems (the "anti-magnetars"; Halpern & Gotthelf 2010), might be of a magnetar that had a strong SN fall-back accretion in the past, and now it spins-down via typical dipolar loss but with a long spin period due to the severe slow down in its early phases (< few hundreds years). In particular, if 1E161348–5055 is born with a magnetic field and spin period such that when the fall back accretion starts the source is at its equilibrium period (Illarionov & Sunyaev 1975), then such accretion will not reach the surface but in the first years or more of its lifetime, the magnetar will stay in the propeller regime (hence with a substantially larger torque than if in the ejector phase). When the fall-back accretion stops, the magnetar continue evolving as any other isolated pulsars, but with a substantially slower spin period. We leave the detailed theoretical calculations of this scenario to a subsequent paper in preparation.

This scenario easily unifies objects as young magnetars, CCOs, or RCW103 as being formed similarly with an initial magnetic field of $B_{\text{birth}} \sim 10^{14-15}$ G, but depending on the exact initial magnetic field intensity, the proto-NS spin period, and the fall-back accretion rate of each SN explosion, direct surface accretion might take place burying the magnetic field in the crust creating the 'hidden-magnetar' CCOs, or the newly born NS might start in the propeller regime soon after birth, resulting in a severe slow-down of its initial spin period at birth. The latter might have been the case of the CCO in RCW103.

ACKNOWLEDGEMENTS

We are grateful to Dr. Belinda Wilkes and Dr. Fiona Harrison for accepting our Director Discretionary Time requests, and to the *Chandra* and *NuSTAR* teams for the large efforts in scheduling these simultaneous observations on such a short timescale. We also acknowledge the *Swift* team for promptly announce new transient events, allowing rapid follow-up observations. NR, AB, PE and FCZ acknowledge funding in the framework of the NWO Vidi award A.2320.0076 (PI: N. Rea), and via the European COST Action MP1304 (NewCOMP-

STAR). NR is also supported by grants AYA2015-71042-P and SGR2014-1073. We acknowledge José A. Pons for useful discussions and valuable comments.

REFERENCES

- Archibald, R. F., Kaspi, V. M., Ng, C.-Y., et al. 2015, *ApJ*, 800, 33
- Beloborodov, A. M. 2009, *ApJ*, 703, 1044
- Bhadkamkar H., Ghosh P., 2009, *A&A*, 506, 1297
- Buccheri R. et al., 1983, *A&A*, 128, 245
- Carter L. M., Dickel J. R., Bomans D. J., 1997, *PASP*, 109, 990
- Caswell J. L., Murray J. D., Roger R. S., Cole D. J., Cooke D. J., 1975, *A&A*, 45, 239
- Chatterjee, P., Hernquist, L., & Narayan, R. 2000, *ApJ*, 534, 373
- D’Ai, A., Gehrels, N., Gronwall, C., et al. 2016, *GCN Circ.*, 19547
- Davis, J. E. 2001, *ApJ*, 562, 575
- De Luca A., Caraveo P. A., Mereghetti S., Tiengo A., Bignami G. F., 2006, *Science*, 313, 814
- De Luca A., Mignani R. P., Zaggia S., Beccari G., Mereghetti S., Caraveo P. A., Bignami G. F., 2008, *ApJ*, 682, 1185
- Duncan, R. C., & Thompson, C. 1992, *ApJ*, 392, L9
- Esposito P., Turolla R., de Luca A., Israel G. L., Possenti A., Burrows D. N., 2011, *MNRAS*, 418, 170
- Frank K. A., Burrows, D. N., Park S., 2015, *ApJ*, 810, 113
- Fruscione A. et al., 2006, in Silva D. R., Doxsey R. E., eds, *Proc. SPIE*, Vol. 6270, *Observatory Operations: Strategies, Processes, and Systems*. SPIE, Bellingham, p. 62701V
- Garmire G. P., Pavlov G. G., Garmire A. B., Zavlin V. E. 2000, *IAU Circ.* 7350
- Garmire G. P., Bautz M. W., Ford P. G., Nousek J. A., Ricker G. R., Jr, 2003, in Truemper J. E., Tananbaum H. D., eds, *Proc. SPIE*, Vol. 4851, *X-Ray and Gamma-Ray Telescopes and Instruments for Astronomy*. SPIE, Bellingham, p. 28
- Halpern, J. P., & Gotthelf, E. V. 2010, *ApJ*, 709, 436
- Harrison, F. A., Craig, W. W., Christensen, F. E., et al. 2013, *ApJ*, 770, 103
- Illarionov, A. F., & Sunyaev, R. A. 1975, *A&A*, 39, 185
- Israel, G. L., & Stella, L. 1996, *ApJ*, 468, 369
- Israel G. L. et al., 2008, *ApJ*, 685, 1114
- Kuiper, L., Hermsen, W., den Hartog, P. R., & Urama, J. O. 2012, *ApJ*, 748, 133
- Li X.-D., 2007, *ApJ*, 666, L81
- Liu, X. W., Xu, R. X., van den Heuvel, E. P. J., et al. 2015, *ApJ*, 799, 233
- Mereghetti, S. 2008, *A&A Rev.*, 15, 225
- Moretti A. et al., 2005, in Siegmund O. H. W., ed., *UV, X-Ray, and Gamma-Ray Space Instrumentation for Astronomy XIV* Vol. 5898 of SPIE Conference Series. SPIE, Bellingham, pp 348-356
- Perna, R., & Pons, J. A. 2011, *ApJ*, 727, L51
- Perna, R., Duffell, P., Cantiello, M., & MacFadyen, A. I. 2014, *ApJ*, 781, 119
- Pizzolato F., Colpi M., De Luca A., Mereghetti S., Tiengo A., 2008, *ApJ*, 681, 530
- Pons, J. A., & Rea, N. 2012, *ApJ*, 750, L6
- Pons J. A., Viganò D., Rea N., 2013, *NatPh*, 9, 431
- Popov S. B., Kurov A. A., Kaminker A. D., 2015, *PASA*, 32, 18
- Rea, N., Israel, G. L., Turolla, R., et al. 2009, *MNRAS*, 396, 2419
- Rea N., Esposito P., 2011, in Torres D. F., Rea N., eds, *Astrophysics and Space Science Proceedings, High-Energy Emission from Pulsars and Their Systems*. Springer-Verlag, Berlin, p. 247
- Rea, N., Israel, G. L., Pons, J. A., et al. 2013, *ApJ*, 770, 65
- Rodríguez Castillo, G. A., Israel, G. L., Esposito, P., et al. 2014, *MNRAS*, 441, 1305
- Tueller J. et al., 2010, *ApJS*, 186, 378
- Turolla, R., Zane, S., & Watts, A. L. 2015, *Reports on Progress in Physics*, 78, 116901
- Viganò, D., Rea, N., Pons, J. A., et al. 2013, *MNRAS*, 434, 123